Journal of Computational Physics 489 (2023) 112255

Contents lists available at ScienceDirect

Journal of Computational Physics

journal homepage: www.elsevier.com/locate/jcp

Energy-conserving successive multi-stage method for the linear wave equation with forcing terms

Jaemin Shin [a], June-Yub Lee [b,*]

[a] Department of Mathematics, Chungbuk National University, Cheongju 28644, Korea
[b] Department of Mathematics, Ewha Womans University, Seoul 03760, Korea

ARTICLE INFO

Article history:
Received 30 August 2022
Received in revised form 26 March 2023
Accepted 28 May 2023
Available online 2 June 2023

Keywords:
Non-homogeneous linear wave equation
High-order method
Energy conservation
Runge–Kutta method
Successive multi-stage method

ABSTRACT

We propose a high-order time-discretized method for a non-homogeneous linear wave equation with a forcing term. The method conserves the accumulated discrete energy with the external term. We provide detailed proofs of unique solvability and unconditional energy conservation of the proposed successive multi-stage (SMS) method. We also present reduced order conditions up to the fourth order with aid of some important algebraic identities from the features of the SMS methods. We demonstrate the accuracy and stability of the SMS methods using numerical experiments. In addition, to show the applicability of the proposed method, we extend the method to solve quasi-linear wave equations and provide numerical simulations for sine-Gordon and Boussinesq-type equations.

1. Introduction

Hyperbolic differential equations arise in many scientific disciplines to model wave propagation phenomena. Among them, linear wave equations play an important role in physics and scientific modeling: acoustic and elastic dynamics for sound and vibration analyses. One of the most famous properties of wave propagation is that the flow has energy conservation. Therefore, to effectively represent the underlying physical phenomenon, we require an accurate numerical scheme with appropriate energy preservation.

A non-homogeneous linear wave equation can be represented as

$$\frac{\partial^2 u}{\partial t^2} = \nabla \cdot (\mathbf{M}(\mathbf{x})\nabla u) + f(\mathbf{x}, t), \tag{1}$$

with a variable coefficient matrix $\mathbf{M}(\mathbf{x})$ and external force $f(\mathbf{x}, t)$ in the domain $\Omega \subset \mathbb{R}^d$ $(d = 1, 2, 3)$. Assuming that the coefficient $\mathbf{M}(\mathbf{x})$ is a symmetric positive definite matrix, the corresponding energy functional is defined as follows:

$$\mathcal{F}(t) = \int_\Omega \left(\frac{1}{2}\left(\frac{\partial u}{\partial t}\right)^2 + \frac{1}{2}\left|\sqrt{\mathbf{M}(\mathbf{x})}\nabla u\right|^2 - \int_0^t f(\mathbf{x}, \tau)\, \frac{\partial u}{\partial \tau}(\mathbf{x}, \tau)\, d\tau \right) d\mathbf{x}, \tag{2}$$

* Corresponding author.
E-mail address: jyllee@ewha.ac.kr (J.-Y. Lee).

https://doi.org/10.1016/j.jcp.2023.112255
0021-9991/

where the l_2-norm $\left|\sqrt{\mathbf{M}(\mathbf{x})}\nabla u\right|$ is given by an inner product $(\nabla u, \mathbf{M}(\mathbf{x})\nabla u)^{1/2}$. Equation (1) can be completed with initial and boundary conditions. In this study, we take periodic or zero Neumann boundary conditions for the sake of simplicity. Note that the solution of the wave equation satisfies the energy conservation property,

$$\frac{d}{dt}\mathcal{F}(t) = \int_{\Omega}\left(\frac{\partial^2 u}{\partial t^2} - \nabla\cdot(\mathbf{M}(\mathbf{x})\nabla u) - f(\mathbf{x},t)\right)\frac{\partial u}{\partial t}\,d\mathbf{x} = 0. \tag{3}$$

Various studies have been conducted on developing an energy-conserving high-order method for homogeneous linear wave equations. For example, the theta method [1] achieves energy stability by generalizing the leap-frog method [2], which is a well-known multi-step method used for many applications but does not guarantee stability with larger time steps. The Crank–Nicolson method is another well-known second-order example that guarantees energy conservation for the wave equation. Based on this, many studies aim to find a higher-order energy-conserving method [3–6]. On the other hand, the numerical treatment of Hamiltonian partial differential equations has been an intensive research area over the past decade; for example, the symplectic Runge–Kutta (RK) method [7–9], average vector field method [10–12], discrete variational derivative methods [13,14], and Hamiltonian boundary value method [15]. These studies focused on finding conditions for energy conservation in RK methods. Despite the remarkable numerical methods with high-order accuracy and energy conservation, the extension to a linear equation with external force has rarely been discussed. Most studies point to the semilinear and nonlinear wave equations instead. However, the non-homogeneous term that varies in space and time is practically valuable to physical modeling.

In this study, we present a high-order energy-preserving scheme for the non-homogeneous linear wave equation (1). The successive multi-stage (SMS) method, which was originally proposed in [16], guarantees energy conservation for the homogeneous linear wave equation without the source term, $f \equiv 0$. It is a high-order extension of the well-known second-order Crank–Nicolson method using the RK framework, but we have shown [16] that the SMS method is not an example of symplectic RK methods. To generalize the original SMS method for more general cases with the external forcing term, we must discuss the extended order conditions, which create a complicated system of multi variate high-order polynomial equations, unlike the homogeneous case. To handle this problem, we develop a systematic approach to reduce the number of order conditions. We also remark that the purpose of this study is not only to present a general SMS method for non-homogeneous linear wave equations but also demonstrate the applicability of the proposed method beyond the linear equation.

In Section 2, we extend the Crank–Nicolson method to design a new high-order implicit scheme that is unconditionally energy conserved. This idea of using RK framework is similar to that in [16], but we redo the proofs of unique solvability and energy conservation with the forcing term for the self-consistency of this study. In Section 3, we present basic identities on the variables in the RK Butcher table and a systematic approach for finding RK tables for the second-, third-, and fourth-order accurate SMS methods. We present numerical examples to demonstrate the order of convergence and energy conservation of the SMS methods in Section 4. Although the SMS method is designed for the linear wave equation with forcing terms, it can be used for more general cases, such as quasi-linear wave equations. The numerical simulations in Section 5 suggest the applicability of the high-order SMS methods, although energy conservation is no longer valid. In Section 6, we conclude the paper with a remark on future studies for high-order energy conserving methods for general Hamiltonian systems.

2. Successive multi-stage methods

By defining an auxiliary variable $v = u_t$, we can represent the linear wave equation (1) in a decoupled form:

$$\begin{aligned}\frac{\partial u}{\partial t} &= v,\\ \frac{\partial v}{\partial t} &= \nabla\cdot(\mathbf{M}(\mathbf{x})\nabla u) + f(\mathbf{x},t),\end{aligned} \tag{4}$$

where we take periodic or zero Neumann boundary conditions. The system can be evolved with initial conditions $u(\mathbf{x},0) = u_0(\mathbf{x})$, $v(\mathbf{x},0) = \frac{\partial u}{\partial t}(\mathbf{x},0) = v_0(\mathbf{x})$. Then, the energy $\mathcal{F}(t)$ in (2) can be redefined as

$$\mathcal{H}(u,v) = \int_{\Omega}\left(\frac{1}{2}v^2 + \frac{1}{2}\left|\sqrt{\mathbf{M}(\mathbf{x})}\nabla u\right|^2 - \int_0^t f(\mathbf{x},\tau)\,v(\mathbf{x},\tau)\,d\tau\right)d\mathbf{x}. \tag{5}$$

First, we denote u^n and v^n as the approximations of u and v at time $t^n = n\Delta t$, respectively. We now consider the well-known Crank–Nicolson method as

$$\begin{aligned}\frac{u^{n+1}-u^n}{\Delta t} &= \frac{v^{n+1}+v^n}{2},\\ \frac{v^{n+1}-v^n}{\Delta t} &= \nabla\cdot\left(\mathbf{M}(\mathbf{x})\nabla\frac{u^{n+1}+u^n}{2}\right) + \frac{f^{n+1}+f^n}{2},\end{aligned} \tag{6}$$

where $f^n = f\left(\mathbf{x}, t^n\right)$. The corresponding semi-discrete energy can be defined as

$$\mathcal{H}\left(u^n, v^n\right) = \int_\Omega \frac{1}{2}\left(v^n\right)^2 + \frac{1}{2}\left|\sqrt{\mathbf{M}(\mathbf{x})}\nabla u^n\right|^2 - \frac{\Delta t}{4}\sum_{k=1}^{n}\left(f^k + f^{k-1}\right)\left(v^k + v^{k-1}\right) d\mathbf{x}. \tag{7}$$

Here, $\frac{\Delta t}{4}\sum_{k=1}^{n}\left(f^k + f^{k-1}\right)\left(v^k + v^{k-1}\right)$ is the Crank–Nicolson summation of the energy induced by the forcing term, $\int_0^{t^n} f\left(\mathbf{x}, \tau\right) v\left(\mathbf{x}, \tau\right) d\tau$.

Theorem 1. *The Crank–Nicolson method (6) is unconditionally energy conserving, meaning that, for any time step size Δt,*

$$\mathcal{H}\left(u^{n+1}, v^{n+1}\right) = \mathcal{H}\left(u^n, v^n\right). \tag{8}$$

Proof. We first calculate the difference of energy functionals:

$$\begin{aligned}\mathcal{H}\left(u^{n+1}, v^{n+1}\right) - \mathcal{H}\left(u^n, v^n\right) = \frac{1}{2}\int_\Omega \left(v^{n+1}\right)^2 - \left(v^n\right)^2 + \left|\sqrt{\mathbf{M}(\mathbf{x})}\nabla u^{n+1}\right|^2 - \left|\sqrt{\mathbf{M}(\mathbf{x})}\nabla u^n\right|^2 \\ - \frac{\Delta t}{2}\left(f^{n+1} + f^n\right)\left(v^{n+1} + v^n\right) d\mathbf{x}.\end{aligned} \tag{9}$$

For the first two terms and the last term in the integrand of (9), we can rearrange as follows:

$$\begin{aligned}&\frac{1}{2}\int_\Omega \left(v^{n+1}\right)^2 - \left(v^n\right)^2 - \frac{\Delta t}{2}\left(f^{n+1} + f^n\right)\left(v^{n+1} + v^n\right) d\mathbf{x} \\ &\quad = \frac{1}{2}\int_\Omega \left(v^{n+1} - v^n\right)\left(v^{n+1} + v^n\right) - \frac{\Delta t}{2}\left(f^{n+1} + f^n\right)\left(v^{n+1} + v^n\right) d\mathbf{x} \\ &\quad = \frac{\Delta t}{4}\int_\Omega \left(v^{n+1} + v^n\right)\nabla\cdot\left(\mathbf{M}(\mathbf{x})\nabla\left(u^{n+1} + u^n\right)\right) d\mathbf{x} \\ &\quad = -\frac{\Delta t}{4}\int_\Omega \nabla\left(v^{n+1} + v^n\right)\cdot\left(\mathbf{M}(\mathbf{x})\nabla\left(u^{n+1} + u^n\right)\right) d\mathbf{x}.\end{aligned} \tag{10}$$

Moreover, for the middle two terms of (9), we can expand as follows:

$$\begin{aligned}&\frac{1}{2}\int_\Omega \left|\sqrt{\mathbf{M}(\mathbf{x})}\nabla u^{n+1}\right|^2 - \left|\sqrt{\mathbf{M}(\mathbf{x})}\nabla u^n\right|^2 d\mathbf{x} \\ &\quad = \frac{1}{2}\int_\Omega \nabla\left(u^{n+1} - u^n\right)\cdot\left(\mathbf{M}(\mathbf{x})\nabla\left(u^{n+1} + u^n\right)\right) d\mathbf{x} \\ &\quad = \frac{\Delta t}{4}\int_\Omega \nabla\left(v^{n+1} + v^n\right)\cdot\left(\mathbf{M}(\mathbf{x})\nabla\left(u^{n+1} + u^n\right)\right) d\mathbf{x}.\end{aligned} \tag{11}$$

Adding (10) and (11), we obtain

$$\mathcal{H}\left(u^{n+1}, v^{n+1}\right) - \mathcal{H}\left(u^n, v^n\right) = 0. \tag{12}$$

Therefore, we can prove that the energy corresponding to the numerical solution $\left(u^n, v^n\right)$ of the Crank–Nicolson method remains a physical constant $\mathcal{F}(t)$,

$$\mathcal{H}\left(u^n, v^n\right) = \mathcal{H}\left(u^0, v^0\right) = \mathcal{F}\left(t^0\right), \tag{13}$$

for any time step Δt. □

We now extend an SMS method [16] to the forced linear wave equation, which is a high-order energy conserving numerical scheme.

Algorithm 1 *(SMS).* For a given coefficient vector

$$R_s = [r_1, r_2, \cdots, r_s], \tag{14}$$

the SMS(R_s) method computes $\left(u^{n+1}, v^{n+1}\right)$ at $t^{n+1} = t^n + \Delta t$. Starting with

$$u_0 = u^n,\ v_0 = v^n$$

for the initial stage, we evaluate (u_i, v_i) for $i = 1, 2, \cdots, s$ by solving

$$\begin{aligned} \frac{u_i - u_{i-1}}{\Delta t} &= r_i \left(v_i + v_{i-1}\right), \\ \frac{v_i - v_{i-1}}{\Delta t} &= r_i \nabla \cdot \left(\mathbf{M}(\mathbf{x}) \nabla \left(u_i + u_{i-1}\right)\right) + r_i \left(f_i + f_{i-1}\right), \end{aligned} \tag{15}$$

where $f_i = f\left(\mathbf{x}, t^n + c_i \Delta t\right)$. Then, the next time step approximations are given by

$$u^{n+1} = u_s,\ v^{n+1} = v_s.$$

2.1. Unique solvability

Theorem 2. *The proposed SMS method (15) is uniquely solvable for any time step size Δt, provided that f depends only on x and t.*

Proof. For each stage $i = 1, 2, \cdots, s$, we must solve

$$\begin{aligned} &u_i - r_i \Delta t\, v_i = u_{i-1} + r_i \Delta t\, v_{i-1}, \\ &v_i - r_i \Delta t \nabla \cdot \left(\mathbf{M}(\mathbf{x}) \nabla u_i\right) = v_{i-1} + r_i \Delta t \nabla \cdot \left(\mathbf{M}(\mathbf{x}) \nabla u_{i-1}\right) + r_i \Delta t \left(f_i + f_{i-1}\right). \end{aligned} \tag{16}$$

System (16) can be represented as

$$u_i - r_i^2 \Delta t^2 \nabla \cdot \left(\mathbf{M}(\mathbf{x}) \nabla u_i\right) = \chi_i + r_i^2 \Delta t^2 \left(f_i + f_{i-1}\right), \tag{17}$$

where

$$\chi_i = u_{i-1} + 2 r_i \Delta t\, v_{i-1} + r_i^2 \Delta t^2 \nabla \cdot \left(\mathbf{M}(\mathbf{x}) \nabla u_{i-1}\right). \tag{18}$$

Because $\mathbf{M}(\mathbf{x})$ is a symmetric positive definite matrix and $I - r_i^2 \Delta t^2 \nabla \cdot (\mathbf{M}(\mathbf{x}) \nabla)$ is an invertible operator, (17) has a unique solution for any time step Δt. Using the solution u_i of (17), we can easily obtain a unique solution v_i using (16). □

Remark 1. The SMS method is an implicit RK scheme which is computationally more expensive than an explicit RK method. Theorem 2 implies unique solvability of the implicit equation (16) and the proposed method has a unique novelty for inheriting the energy conservation property to the forced linear wave equation, which will be shown in next subsection.

2.2. Energy conservation

Now, the semi-discrete energy can be defined as

$$\mathcal{H}^{\Delta t}\left(u^n, v^n\right) = \int_\Omega \left(\frac{1}{2} \left(v^n\right)^2 + \frac{1}{2} \left| \sqrt{\mathbf{M}(\mathbf{x})} \nabla u^n \right|^2 \right) d\mathbf{x} - \frac{\Delta t}{2} \sum_{k=0}^{n-1} \sum_{p=1}^{s} \sigma_p^k, \tag{19}$$

where

$$\sigma_p^k = r_p \int_\Omega \left(f_p^k + f_{p-1}^k\right) \left(v_p^k + v_{p-1}^k\right) d\mathbf{x}. \tag{20}$$

Note that $\frac{\Delta t}{2} \sum_{k=0}^{n-1} \sum_{p=1}^{s} \sigma_p^k$ is the Runge–Kutta summation of the energy induced by the forcing term, $\int_0^{t^n} \int_\Omega f(\mathbf{x}, \tau) v(\mathbf{x}, \tau)\, d\mathbf{x}\, d\tau$.

Theorem 3. *For each intermediate stage of the proposed SMS method (15) with $(u_0, v_0) = (u^n, v^n)$, we can extend the discrete energy (19) as follows:*

$$\mathcal{H}^{\Delta t}\left(u_i, v_i\right) = \int_\Omega \left(\frac{1}{2} \left(v_i\right)^2 + \frac{1}{2} \left| \sqrt{\mathbf{M}(\mathbf{x})} \nabla u_i \right|^2 \right) d\mathbf{x} - \frac{\Delta t}{2} \left(\sum_{k=0}^{n-1} \sum_{p=1}^{s} \sigma_p^k + \sum_{p=1}^{i} \sigma_p^n \right).$$

Then, the discrete energy between adjacent stages is conserved for any time step $r_i\Delta t$,

$$\mathcal{H}^{\Delta t}(u_i, v_i) = \mathcal{H}^{\Delta t}(u_{i-1}, v_{i-1}). \tag{21}$$

Finally, the proposed method (15) is unconditionally energy conserving, meaning that $\mathcal{H}^{\Delta t}\left(u^{n+1}, v^{n+1}\right) = \mathcal{H}^{\Delta t}\left(u^n, v^n\right)$ for any time step Δt.

Proof. Similar to the proof of Theorem 1, we first arrange the difference of adjacent discrete energy functionals,

$$\begin{aligned}\mathcal{H}^{\Delta t}(u_i, v_i) - \mathcal{H}^{\Delta t}(u_{i-1}, v_{i-1}) = \frac{1}{2}\int_\Omega v_i^2 - v_{i-1}^2 + \left|\sqrt{\mathbf{M}(\mathbf{x})}\nabla u_i\right|^2 - \left|\sqrt{\mathbf{M}(\mathbf{x})}\nabla u_{i-1}\right|^2 \\ - r_i\Delta t\,(v_i + v_{i-1})\,(f_i + f_{i-1})\,d\mathbf{x}.\end{aligned} \tag{22}$$

We can then expand the separated terms of (22) as

$$\begin{aligned}&\frac{1}{2}\int_\Omega v_i^2 - v_{i-1}^2 - r_i\Delta t\,(v_i + v_{i-1})\,(f_i + f_{i-1})\,d\mathbf{x} \\ &\qquad = -\frac{r_i\Delta t}{2}\int_\Omega \nabla(v_i + v_{i-1})\cdot(\mathbf{M}(\mathbf{x})\nabla(u_i + u_{i-1}))\,d\mathbf{x},\end{aligned} \tag{23}$$

$$\begin{aligned}&\frac{1}{2}\int_\Omega \left|\sqrt{\mathbf{M}(\mathbf{x})}\nabla u_i\right|^2 - \left|\sqrt{\mathbf{M}(\mathbf{x})}\nabla u_{i-1}\right|^2 d\mathbf{x} \\ &\qquad = \frac{r_i\Delta t}{2}\int_\Omega \nabla(v_i + v_{i-1})\cdot(\mathbf{M}(\mathbf{x})\nabla(u_i + u_{i-1}))\,d\mathbf{x}.\end{aligned} \tag{24}$$

Now, we have $\mathcal{H}^{\Delta t}(u_i, v_i) = \mathcal{H}^{\Delta t}(u_{i-1}, v_{i-1})$ for any $r_i\Delta t$, $i = 1, 2, \cdots, s$. Therefore,

$$\mathcal{H}^{\Delta t}\left(u^{n+1}, v^{n+1}\right) = \mathcal{H}^{\Delta t}(u_s, v_s) = \mathcal{H}^{\Delta t}(u_0, v_0) = \mathcal{H}^{\Delta t}\left(u^n, v^n\right), \tag{25}$$

which proves the conservation of the discrete energy functional $\mathcal{H}^{\Delta t}\left(u^n, v^n\right)$. □

3. Order conditions for temporal accuracy

Note that the SMS(R_1) with $R_1 = \left[\frac{1}{2}\right]$ is identical to the Crank–Nicolson method and provides the second-order accuracy. To construct a high-order method, we introduce a framework of Runge–Kutta (RK) method to explain the time accuracy for the successive multi-stage method. As in [16], we can describe the s-stage SMS method (15) using a Butcher table:

$$\begin{array}{c|c} \mathbf{c} & \mathbf{A} \\ \hline & \mathbf{b}^T \end{array} = \begin{array}{c|ccccc} 0 & 0 & 0 & 0 & \cdots & 0 \\ c_1 & r_1 & r_1 & 0 & \cdots & 0 \\ c_2 & r_1 & r_1 + r_2 & r_2 & \cdots & 0 \\ \vdots & \vdots & \vdots & \vdots & \ddots & \vdots \\ c_s & r_1 & r_1 + r_2 & r_2 + r_3 & \cdots & r_s \\ \hline & r_1 & r_1 + r_2 & r_2 + r_3 & \cdots & r_s \end{array} \tag{26}$$

where $\mathbf{A} \in \mathbb{R}^{(s+1)\times(s+1)}$, $\mathbf{b} \in \mathbb{R}^{s+1}$, and $\mathbf{c} = \mathbf{A}\mathbf{1}$ with $\mathbf{1} = (1, 1, \ldots, 1)^T \in \mathbb{R}^{s+1}$. Note that the last row of the coefficient matrix $\mathbf{A}$ is identical to the evaluation vector $\mathbf{b}$, which is known as a stiffly accurate condition.

Table 1 lists the order conditions of the Runge–Kutta method up to fourth-order accuracy. For more information, we refer to [17,18]. Because the SMS method (15) is not homogeneous, we must consider all the order conditions of the RK method for the desired order accuracy.

We may require more stages to find an SMS method that satisfies all of these conditions compared with the SMS methods [16] for the linear and autonomous system. However, by the following simple and useful lemmas, we can dramatically reduce the number of the required order conditions.

Lemma 4. *The tables with* $\mathbf{A}$, $\mathbf{b}$, *and* $\mathbf{c}$ *for the SMS method (15) satisfy the following equality,* $\mathbf{c}^2 = 2\mathbf{A}\mathbf{c}$.

Table 1
Order conditions of RK methods up to the fourth-order accuracy. Here, $\odot$ denotes component-wise multiplication of two vectors and $\mathbf{c}^n = \mathbf{c}^{n-1} \odot \mathbf{c}$.

order	1	2	3	4
condition	$\mathbf{b}^T\mathbf{1} = 1$	$\mathbf{b}^T\mathbf{c} = 1/2$	$\mathbf{b}^T\mathbf{Ac} = 1/6$ $\mathbf{b}^T\mathbf{c}^2 = 1/3$	$\mathbf{b}^T\mathbf{A}^2\mathbf{c} = 1/24$ $\mathbf{b}^T\mathbf{Ac}^2 = 1/12$ $\mathbf{b}^T(\mathbf{c} \odot \mathbf{Ac}) = 1/8$ $\mathbf{b}^T\mathbf{c}^3 = 1/4$

Table 2
Reduced order conditions up to the fourth-order accuracy.

order	1	2	3	4
condition	$\mathbf{b}^T\mathbf{1} = 1$	$\mathbf{b}^T\mathbf{c} = 1/2$	$\mathbf{b}^T\mathbf{Ac} = 1/6$	$\mathbf{b}^T\mathbf{A}^2\mathbf{c} = 1/24$ $\mathbf{b}^T\mathbf{c}^3 = 1/4$

Proof. The i-th components of $\mathbf{c}$ and $\mathbf{Ac}$ can be written as follows:

$$\mathbf{c}_i = 2\sum_{j=1}^{i} r_j, \tag{27}$$

$$(\mathbf{Ac})_i = \sum_j a_{ij}c_j = \sum_{j=1}^{i-1} \left(r_j + r_{j+1}\right) c_j + r_i c_i. \tag{28}$$

Clearly, $2\,(\mathbf{Ac})_1 = 2r_1c_1 = c_1^2$. Let us use a mathematical induction starting with

$$2\,(\mathbf{Ac})_i = 2\sum_{j=1}^{i-1} \left(r_j + r_{j+1}\right) c_j + 2r_i c_i = c_i^2. \tag{29}$$

Because $c_{i+1} = c_i + 2r_{i+1}$, we have

$$\begin{aligned} 2\,(\mathbf{Ac})_{i+1} &= 2\sum_{j=1}^{i} \left(r_j + r_{j+1}\right) c_j + 2r_{i+1}c_{i+1} \\ &= 2\sum_{j=1}^{i-1} \left(r_j + r_{j+1}\right) c_j + 2r_i c_i + 2r_{i+1}c_i + 2r_{i+1}\left(c_i + 2r_{i+1}\right) \\ &= c_i^2 + 4r_{i+1}c_i + 4r_{i+1}^2 = (c_i + 2r_{i+1})^2 = c_{i+1}^2. \quad \square \end{aligned} \tag{30}$$

By Lemma 4, we can simplify the order conditions, and Table 2 lists the reduced order conditions. We should note that only one condition $\mathbf{b}^T\mathbf{c}^3 = 1/4$ is additionally involved compared with the linear RK method; see the appendix in [16].

We define a lower triangular matrix L as $l_{ij} = 1$ if $i > j$, and 0 otherwise. For simplicity, we define $r_0 = 0$. Then, we can represent the coefficient matrix $\mathbf{A}$ as

$$a_{ij} = l_{ij}b_j + \delta_{ij}r_j, \tag{31}$$

where δ_{ij} is the Kronecker delta function. Furthermore, we can rearrange the multiplication of $\mathbf{b}$ and $\mathbf{A}$ as

$$\left(\mathbf{b}^T\mathbf{A}\right)_j = \sum_i b_i a_{ij} = \sum_i b_i \left(l_{ij}b_j + \delta_{ij}r_j\right) = \left(\sum_{i>j} b_i\right) b_j + r_j b_j \tag{32}$$

and the multiplication of $\mathbf{A}$ and $\mathbf{c}$ as

$$(\mathbf{Ac})_j = \sum_{i<j} b_i c_i + r_j c_j. \tag{33}$$

Lemma 5. *For the SMS method (15), the first-order condition $\mathbf{b}^T\mathbf{1} = 1$ implies that the second-order condition $\mathbf{b}^T\mathbf{c} = 1/2$.*

Proof. Using (32), we first extend it as follows:

$$\begin{aligned}\mathbf{b}^T\mathbf{c} = \left(\mathbf{b}^T\mathbf{A}\right)\mathbf{1} &= \sum_j \left(\sum_i b_i a_{ij}\right) = \sum_{i>j} b_i b_j + \sum_j r_j b_j \\ &= \frac{1}{2}\sum_{i,j} b_i b_j + \frac{1}{2}\sum_j b_j\left(2r_j - b_j\right).\end{aligned} \tag{34}$$

Because

$$\sum_{j=0}^{s} b_j(2r_j - b_j) = -r_1^2 + \sum_{j=1}^{s-1}(r_j^2 - r_{j+1}^2) + r_s^2 = 0, \tag{35}$$

we finally obtain

$$\mathbf{b}^T\mathbf{c} = \frac{1}{2}\sum_{i,j} b_i b_j = \frac{1}{2}\left(\sum_i b_i\right)\left(\sum_j b_j\right), \tag{36}$$

which means that $\mathbf{b}^T\mathbf{1} = \pm 1$ and $\mathbf{b}^T\mathbf{c} = 1/2$ are equivalent. □

Lemma 6. *Suppose that* $\mathbf{b}^T\mathbf{1} = 1$ *is satisfied in the SMS method* (15)*. Then,*

$$\left(\mathbf{b}^T - \mathbf{b}^T\mathbf{A}\right)\mathbf{A}\mathbf{c} = \frac{1}{2}\left(\sum_j c_j b_j\right)\left(\sum_i c_i b_i\right) = \frac{1}{8}. \tag{37}$$

Therefore, $\mathbf{b}^T\mathbf{A}\mathbf{c} = 1/6$ *and* $\mathbf{b}^T\mathbf{A}^2\mathbf{c} = 1/24$ *are equivalent.*

Proof.

$$\begin{aligned}\left(\mathbf{b}^T - \mathbf{b}^T\mathbf{A}\right)_j &= b_j - \left(\sum_{i>j} b_i\right) b_j - r_j b_j = \left(\sum_{i\le j} b_i\right) b_j - r_j b_j \\ &= \left(c_j + r_{j+1}\right) b_j - r_j b_j = c_j b_j + (r_{j+1} - r_j) b_j.\end{aligned} \tag{38}$$

Now, using (33) and (38), we can expand as follows:

$$\begin{aligned}\left(\mathbf{b}^T - \mathbf{b}^T\mathbf{A}\right)\mathbf{A}\mathbf{c} &= \sum_j \left(c_j b_j + \left(r_{j+1} - r_j\right) b_j\right)\left(\sum_{i<j} b_i c_i + r_j c_j\right) \\ &= \frac{1}{2}\left(\sum_j c_j b_j\right)\left(\sum_i c_i b_i\right) - \frac{1}{2}\sum_j c_j^2 b_j^2 \\ &\quad + \sum_j \left(r_{j+1} - r_j\right) b_j \left(\sum_{i<j} b_i c_i + r_j c_j\right) + \sum_j r_j b_j c_j^2 \\ &= \frac{1}{2}\left(\sum_j c_j b_j\right)\left(\sum_i c_i b_i\right).\end{aligned} \tag{39}$$

The last simplification comes from $r_j - b_j/2 = \left(r_j - r_{j+1}\right)/2$, $\sum_{i\le j} b_i c_i = c_j c_{j+1}/2$, and

$$\begin{aligned}&\sum_j b_j \left(r_j c_j^2 - b_j c_j^2/2 + \left(r_{j+1} - r_j\right)\left(\sum_{i<j} b_i c_i + r_j c_j\right)\right) \\ &= \sum_j b_j\left(r_{j+1} - r_j\right)\left(-c_j^2/2 + \sum_{i\le j} b_i c_i - r_{j+1} c_j\right) = 0. \quad \square\end{aligned} \tag{40}$$

Table 3
Reduced order conditions up to the fourth-order accuracy.

order	2	3	4
condition	$\mathbf{b}^T\mathbf{1}=1$	$\mathbf{b}^T\mathbf{Ac}=1/6$	$\mathbf{b}^T\mathbf{c}^3=1/4$

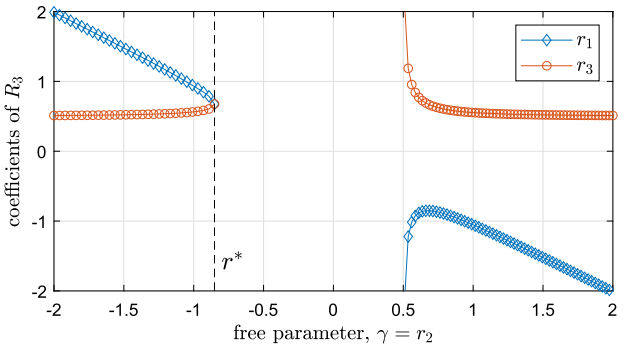

Fig. 1. Coefficients of R_3.

By Lemma 5 and 6, the order conditions in Table 2 can be simplified to those in Table 3. We should recall [16] that the coefficients satisfying up to third-order conditions for the linear wave equation also satisfy the fourth-order condition $\mathbf{b}^T\mathbf{A}^2\mathbf{c}=1/24$. However, with the forcing term, we need to have one additional order condition $\mathbf{b}^T\mathbf{c}^3=1/4$ to obtain the fourth-order accuracy. We remark that the number of order conditions for fifth- or higher-order cases increases dramatically with the forcing term unlike the linear cases in [16] and we will deal with reduction techniques for higher-order cases in another manuscript.

Remark 2. By Lemmas 4 and 5, the order conditions in Table 3 can be written as $\mathbf{b}^T\mathbf{c}=1/2$, $\mathbf{b}^T\mathbf{c}^2=1/3$, and $\mathbf{b}^T\mathbf{c}^3=1/4$ for the second-, third-, and fourth-order accuracies, respectively.

Remark 3. No solution for the two-stage coefficient vector $R_2=[r_1,r_2]$ satisfies the order conditions up to third-order accuracy.

Next, we introduce a process for finding R_3 to construct three-stage SMS methods. We now choose a possible choice of the coefficient vector $R_3=[r_1,r_2,r_3]$ and consider the corresponding matrix $\mathbf{A}$ and vector $\mathbf{b}$ as

$$\mathbf{A}=\begin{bmatrix} 0 & 0 & 0 & 0 \\ r_1 & r_1 & 0 & 0 \\ r_1 & r_1+r_2 & r_2 & 0 \\ r_1 & r_1+r_2 & r_2+r_3 & r_3 \end{bmatrix}, \quad \mathbf{b}=\begin{bmatrix} r_1 \\ r_1+r_2 \\ r_2+r_3 \\ r_3 \end{bmatrix}. \tag{41}$$

To satisfy the second-order condition $\mathbf{b}^T\mathbf{1}=1$, the coefficients should satisfy

$$r_1+r_2+r_3=\frac{1}{2}. \tag{42}$$

With the identity in (42) and the third-order condition $\mathbf{b}^T\mathbf{Ac}=1/6$, we obtain the following identity after some algebraic manipulations,

$$r_1r_2+r_1r_3+r_2r_3-2r_1r_2r_3=\frac{1}{12}. \tag{43}$$

When we set a free parameter $r_2=\gamma$, parameters r_1 and r_3 satisfy

$$r_1+r_3=\frac{1-2\gamma}{2},\ r_1r_3=\frac{1-6\gamma+12\gamma^2}{12\,(1-2\gamma)}. \tag{44}$$

Fig. 1 shows the coefficients of R_3 with respect to the parameter of γ. Note that switching r_1 and r_3 can be another solution because of the symmetry between the two variables. This figure implies that infinitely many three-stage third-order SMS methods exist. In choosing $\gamma=4/5$ for numerical simulation, we have

$$R_3\,(4/5)\approx[0.5993,0.8000,-0.8993]. \tag{45}$$

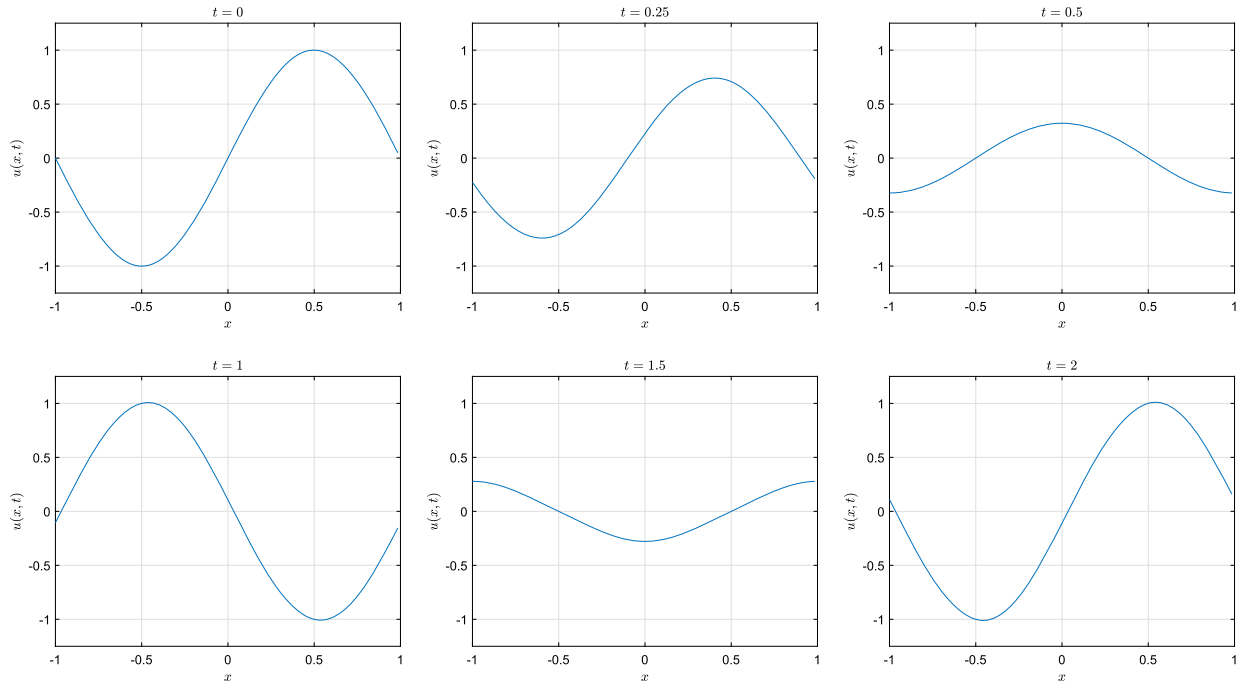

Fig. 2. Evolution of the solution for the 1D wave equation.

There is no solution in $\gamma^* < \gamma \leq 1/2$, where $\gamma^* = -\frac{\sqrt[3]{2}}{3} - \frac{1}{3\sqrt[3]{2}} - \frac{1}{6}$ (approximately -0.8512) is the value that makes r_1 and r_3 the double roots of (44). We observe that the coefficients $R_3(\gamma^*)$ satisfy the order condition $\mathbf{b}^T\mathbf{c}^3 = 1/4$ for the fourth-order accuracy, which is the unique choice for the three-stage fourth-order SMS method.

We remark that a third-order SMS method with $R_3(\gamma)$ has a negative time step for any γ. A negative time step may cause trouble for an energy dissipative case, however, it does not cause a serious problem for an energy-conserving equation which is our main concern in the paper. Especially, the unique solvability of u_i in (17) is always valid regardless of the sign of $r_i \Delta t$.

4. Numerical results

The proposed SMS method can be coupled with a method of lines that first discretizes in space and then solves the resulting system of ordinary differential equations. To focus on the temporal order of convergence and energy conservation, we use the Fourier spectral method for spatial discretization, which provides fully resolved spatial accuracy.

4.1. Time evolution in 1D homogeneous medium

To demonstrate the order of the accuracy and energy conservation property of the proposed scheme, we apply the SMS methods to a one-dimensional wave equation in homogeneous medium,

$$u_{tt} = u_{xx} + \sin\left(\pi t^3\right) \tanh\left(5 - 10\,|x|\right) \tag{46}$$

with a periodic boundary condition and the following initial conditions,

$$u\,(x, 0) = \sin\,(\pi x) \text{ and } u_t\,(x, 0) = \cos\,(\pi x) \tag{47}$$

on the domain $\Omega = [-1, 1]$. For simulation, the Fourier spectral method is used for spatial derivatives in the numerical computations up to time $T_f = 2$. Fig. 2 shows the time evolution of the reference solution of the wave equation (46) using the fourth-order method SMS($R_3(\gamma^*)$) with a sufficiently refined computation grid, $\Delta t = T_f/2^{10}$ and $\Delta x = 1/128$.

We demonstrate the numerical convergence using the same conditions and parameters as those used in the beginning. Fig. 3 shows the relative l_2-errors of numerical solutions for spatial and temporal convergence, where the error is computed by comparing with the reference solution. To estimate the spatial convergence, simulations are performed by varying grid points $8, 12, \cdots, 128$ using the fourth-order method, SMS($R_3\,(\gamma^*)$). As shown, the spatial convergence of the results under the grid refinements is evident. Furthermore, the figure shows that 64 grid points ($\Delta x = 1/32$) provide sufficient spatial accuracy for estimating the temporal convergence. To highlight the numerical convergence results for temporal accuracy,

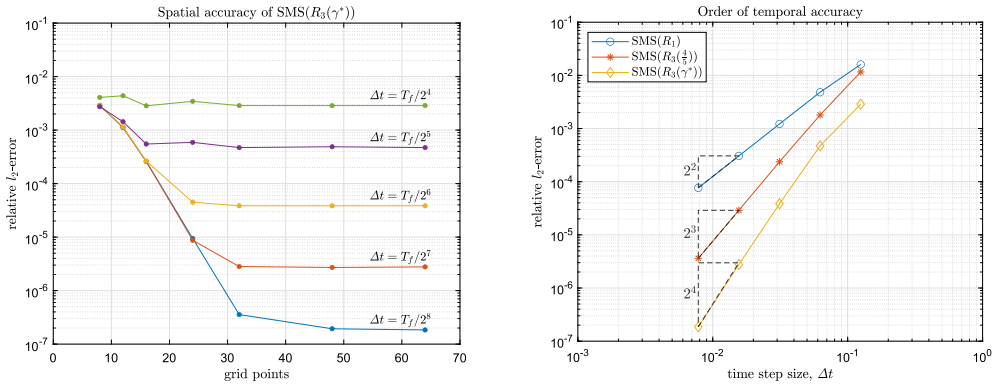

Fig. 3. Relative l_2-errors of solutions at $t = 2$.

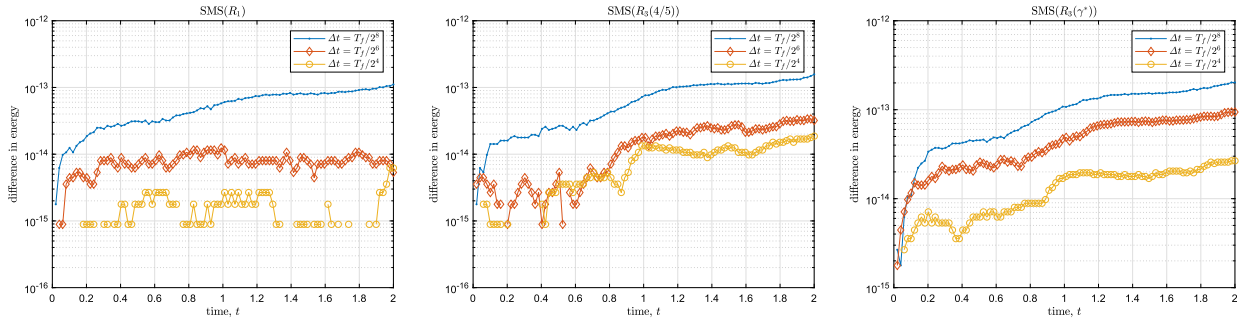

Fig. 4. Evolution of the absolute difference of the discrete energy.

we plot the relative l_2-errors with respect to various time steps $\Delta t = T_f/2^8, \cdots, T_f/2^4$ and a fixed space step $\Delta x = 1/32$. These methods evidently provide the desired order of temporal accuracy.

Fig. 4 shows the time evolution of the difference in the discrete energy defined in (19) for three SMS methods with several time steps. As shown, the energy difference slightly increases because of the accumulation of the random noise error; however, the conservation of the discrete energy is demonstrated under the machine precision. Therefore, the proposed SMS method exhibits discrete energy conservation regardless of the time step size, except for the round-off calculation errors.

4.2. Time evolution in 2D non-homogeneous medium

We present a more complex configuration propagating acoustic pressure, motivated by a numerical example in [1]. We consider a non-homogeneous wave equation with a non-homogeneous medium in a two-dimensional domain,

$$\frac{\partial^2 u}{\partial t^2} = \nabla \cdot (c(x, y) \nabla u) + f(x, y, t), \tag{48}$$

where u is the acoustic pressure, $c(x, y)$ the material properties of the domain of propagation, and $f(x, y, t) = g(x, y) h(t)$ an external source term. Here, the underlying functions are

$$c(x, y) = 1 + 9e^{-0.08\left(x^2+y^2-5^2\right)^2}, \tag{49}$$

$$g(x, y) = e^{-\left((x-1)^2+(y-1)^2\right)}, \tag{50}$$

$$h(t) = \left(50(t-0.7)^2 - 1\right) e^{-25(t-0.7)^2}. \tag{51}$$

Fig. 5 presents the profiles of parameters $c(x, y)$ and $h(t)$. The black dashed circles in the leftmost plot indicate the contour lines at the level of $c(x, y) = 1.01$.

We begin by showing the solution of the wave equation (48) with a zero Neumann boundary condition and the following initial conditions:

$$u(x, y, 0) = 0 \text{ and } u_t(x, y, 0) = 0 \tag{52}$$

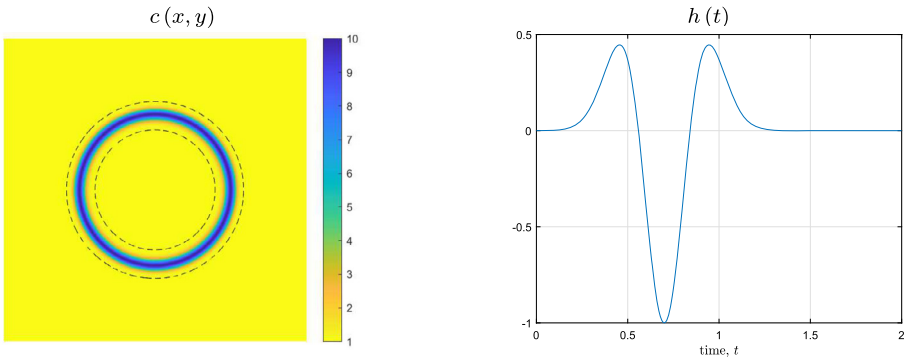

Fig. 5. Representation of the functions $c(x, y)$ and $h(t)$. (For interpretation of the colors in the figures, the reader is referred to the web version of this article.)

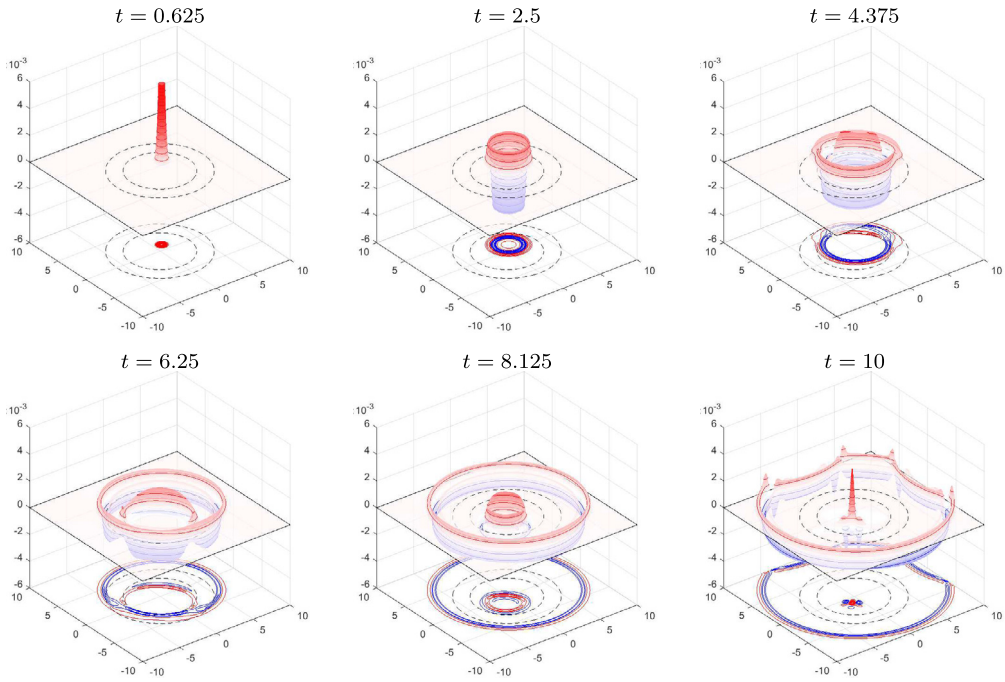

Fig. 6. Evolution of the pressure field.

on a domain $\Omega = [-10, 10] \times [-10, 10]$, and then evolve the system up to a final time $T_f = 10$. Fig. 6 shows the temporal evolution of the pressure field with a sufficiently small time step $\Delta t = T_f/2^{11}$ and $\Delta x = 20/384$ using the fourth-order method, SMS($R_3(\gamma^*)$). These solutions are used as the reference solution to estimate the convergence rate. In each snapshot, we show a 3D plot and its 2D projection on the bottom, where the red and blue regions indicate where u is larger than $5 \cdot 10^{-4}$ and less than $-5 \cdot 10^{-4}$, respectively. To highlight the magnitude, we used red and blue contour lines in increments of $5 \cdot 10^{-4}$. Again, the black dashed circles indicate where the variable coefficient $c(x, y) = 1.01$.

We demonstrate the numerical convergence in space and time with the same conditions and parameters used at the beginning of this subsection. Fig. 7 shows the relative l_2-errors of the solution at $t = 0.625$ with respect to the grid points and time steps. The simulations are performed by varying grid points $N_x = N_y = 64, 96, \cdots, 256$ and time steps $\Delta t = T_f/2^{10}, \cdots, T_f/2^6$. As shown, the spatial convergence of the results under the grid refinements is evident. Furthermore, the figure shows that 256 grid points provide more than a six-digit spatial accuracy to estimate the numerical convergence with respect to the time steps. To highlight the numerical convergence results for temporal accuracy, we plot the relative l_2-errors with respect to the time step with a fixed space step $\Delta x = 20/256$. These methods evidently provide the desired order of temporal accuracy.

Fig. 8 shows the convergence results at $t = 10$, which is quite similar to Fig. 7 except that the convergence order of the SMS($R_3(4/5)$) is higher than 3. Such a super-convergence (of an odd-order numerical method) sometimes occurs when the leading order term in the error equation vanishes.

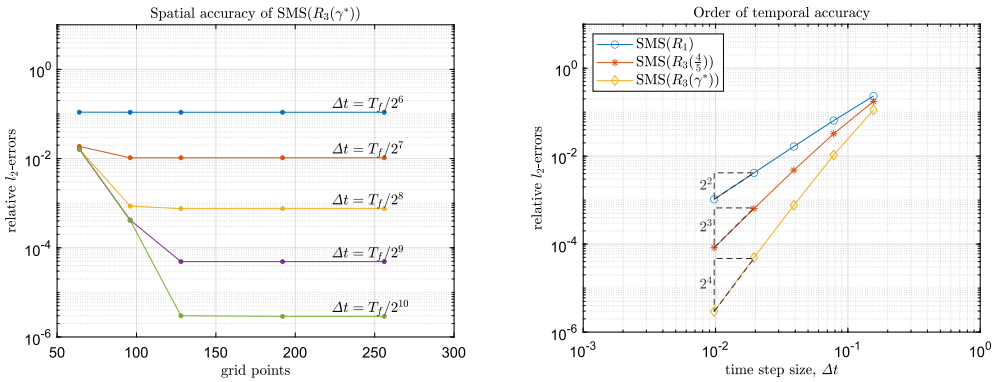

Fig. 7. Relative l_2-errors of solutions at $t = 0.625$.

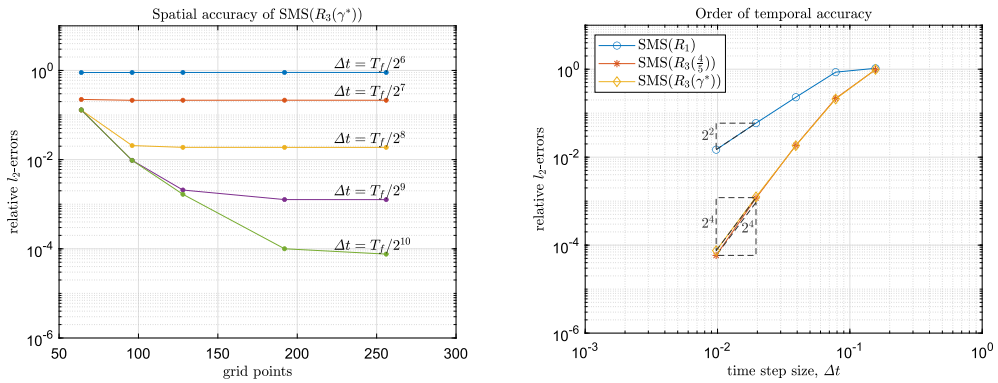

Fig. 8. Relative l_2-errors of solutions at $t = 10$.

5. Extension to quasi-linear equations

Although the SMS method (15) is designed for the linear wave equation with forcing terms (1), it can be applied for more general classes of wave equations. For example, the quasi-linear wave equation

$$\frac{\partial^2 u}{\partial t^2} = \nabla \cdot (\mathbf{M}(\mathbf{x})\nabla u) + f(u) \tag{53}$$

is a system of partial differential equations,

$$\begin{aligned} \frac{\partial u}{\partial t} &= v, \\ \frac{\partial v}{\partial t} &= \nabla \cdot (\mathbf{M}(\mathbf{x})\nabla u) + F'(u), \end{aligned} \tag{54}$$

where the corresponding Hamiltonian functional can be represented as

$$\mathcal{H}_F(u, v) = \int \left(\frac{1}{2} v^2 + \frac{1}{2} \left| \sqrt{\mathbf{M}(\mathbf{x})} \nabla u \right|^2 - F(u) \right) dx. \tag{55}$$

Now, the SMS method (17) for u_i in (54) becomes an implicit equation,

$$u_i - r_i^2 \Delta t^2 \mu_i = \varphi_i, \tag{56}$$

where $\mu_i = \nabla \cdot (\mathbf{M}(\mathbf{x})\nabla u_i) + f(u_i)$ and $\varphi_i = u_{i-1} + 2r_i \Delta t\, v_{i-1} + r_i^2 \Delta t^2 \mu_{i-1}$.

Another example is a system of spatially fourth-order partial differential equations,

$$\begin{aligned} \frac{\partial u}{\partial t} &= v, \\ \frac{\partial v}{\partial t} &= -\Delta \mu, \end{aligned} \tag{57}$$

where $\mu = \nabla \cdot (\mathbf{M}(\mathbf{x})\nabla u) + F'(u)$. Note that (57) can be obtained from the H^{-1} flow of the Hamiltonian functional $\mathcal{H}_F(u, v)$, while (54) from the L^2 flow. Therefore, applying the SMS method for (57) is rather trivial by replacing μ with $-\Delta\mu$. Then, the SMS method becomes an implicit equation,

$$u_i + r_i^2 \Delta t^2 \, \Delta\mu_i = \psi_i, \tag{58}$$

where $\psi_i = u_{i-1} + 2r_i \Delta t \, v_{i-1} - r_i^2 \Delta t^2 \, \Delta\mu_{i-1}$.

The purpose of this section is not to provide an extensive study on the applicability of the SMS method but simply describe using the method beyond the linear wave equation. Thus, we provide only the computational convergence results for a sine-Gordon and Boussinesq-type equations without thorough theoretical analysis.

5.1. Sine-Gordon equation

The sine-Gordon equation is an example of the nonlinear Klein–Gordon equation in the form of (54) the corresponds to the Hamiltonian functional $\mathcal{H}_F(u, v)$ with $F(u) = \cos(u)$ and a homogeneous media $\mathbf{M}(\mathbf{x}) = 1$. Hence, we consider a specific example

$$u_{tt} = \Delta u - \sin u. \tag{59}$$

For the numerical tests, we consider a soliton-like solution [8] in the form of $4\tan^{-1}\left(\varphi(t;\gamma)\,\mathrm{sech}\left(\frac{x}{\gamma}\right)\right)$, where $\varphi(t;\gamma) = \frac{1}{\sqrt{\gamma^2-1}} \sin\left(\frac{\sqrt{\gamma^2-1}}{\gamma} t\right)$. In the special case of $\gamma = 1$, a double-pole solution is provided as follows:

$$u(x, t) = 4\tan^{-1}(t\,\mathrm{sech}\, x). \tag{60}$$

For the numerical test, we set a computational domain $\Omega = [-20, 20]$ and periodic boundary condition. We choose the number of spatial discretization $N_x = 256$ to provide sufficient spatial accuracy and set the initial conditions as $u^0 = u(x, 0)$ and $v^0 = u_t(x, 0)$. For $i = 1, \cdots, s$, we obtain u_i using Newton's method for the nonlinear implicit equation (56),

$$u_i - r_i^2 \Delta t^2 \left(\Delta u_i + f(u_i)\right) = \varphi_i, \tag{61}$$

where $\varphi_i = u_{i-1} + 2r_i \Delta t \, v_{i-1} + r_i^2 \Delta t^2 \left(\Delta u_{i-1} + f(u_{i-1})\right)$. We have an iterative solver for each stage i starting with the previous solution $u_i^{(m=0)} = u^n$:

$$\begin{aligned} u_i^{(m+1)} - r_i^2 \Delta t^2 \, \Delta u_i^{(m+1)} - r_i^2 \Delta t^2 f'\left(u_i^{(m)}\right) u_i^{(m+1)} \\ = \varphi_i + r_i^2 \Delta t^2 \left(f\left(u_i^{(m)}\right) - f'\left(u_i^{(m)}\right) u_i^{(m)}\right). \end{aligned} \tag{62}$$

We terminate the Newton-type m-iteration when the relative consecutive error of $u_i^{(m+1)}$ is less than $tol = 10^{-10}$ and define $u_i = u_i^{(m+1)}$. Then, we have

$$v_i = v_{i-1} + r_i \Delta t \, \Delta\left(u_i + u_{i-1}\right) + r_i \Delta t \, \left(f(u_i) + f(u_{i-1})\right). \tag{63}$$

Finally, we can obtain the next time approximations u^{n+1} and v^{n+1} using u_s and v_s, respectively.

Fig. 9 shows the time evolution of the solution and difference in the Hamiltonian functional up to $T_f = 16$ using the fourth-order SMS($R_3(\gamma^*)$) method. Starting with the zero profile, the evolving speed is fast at the beginning and then slows. For this quasi-linear example, the SMS method no longer guarantees energy conservation. Thus, the energy $\mathcal{H}_F$ associated with the computed solution depends on $\Delta t = T_f/2^{10}, \cdots, T_f/2^5$. Fig. 10 shows the computational solution u^n and energy $\mathcal{H}_F(u^n, v^n)$ associated with the computed solution that converges in the desired order of temporal accuracy. We must remark that the third-order SMS($R_3(4/5)$) method shows super-convergence, as in Fig. 8, but the next example reveals that this is a special case owing to the shape of the solution.

We also consider a superposition of two soliton-like traveling solutions in the form of $4\tan^{-1}\left(e^{(x-x_c-vt)/\sqrt{1-v^2}}\right)$:

$$u(x, t) = 4\tan^{-1}\left(e^{(x-x_1-v_1 t)/\sqrt{1-v_1^2}}\right) - 4\tan^{-1}\left(e^{(x-x_2-v_2 t)/\sqrt{1-v_2^2}}\right), \tag{64}$$

where $(x_1, v_1) = (-20, 0.5)$ and $(x_2, v_2) = (10, 0.25)$. For the numerical test, we set a computational domain $\Omega = [-40, 40]$ with the periodic boundary condition. We then compute the reference solution up to $T_f = 32$ using the fourth-order SMS($R_3(\gamma^*)$) method with $N_x = 256$ and $\Delta t = T_f/2^{11}$. Fig. 11 shows that all SMS methods with $\Delta t = T_f/2^9, \cdots, T_f/2^4$ provide the desired temporal order of accuracy for the computed solution. The convergence order of the Hamiltonian energy at least equals that of the solution.

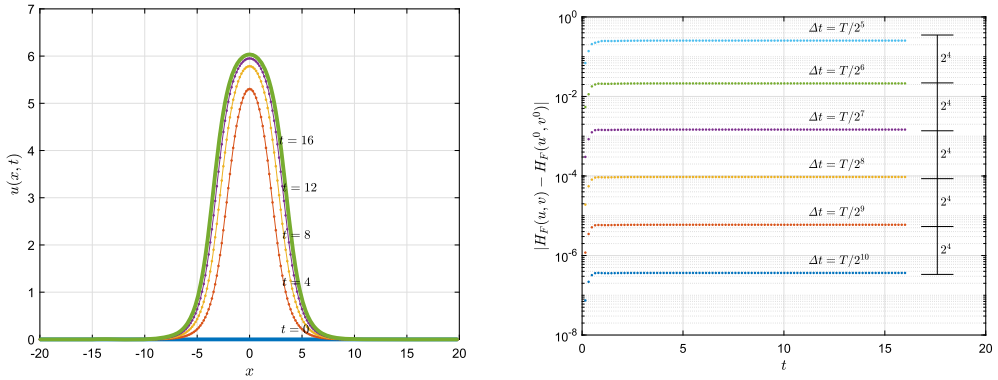

Fig. 9. Evolution of the solution and computational errors of $\mathcal{H}_F(u,v)$ by SMS($R_3(\gamma^*)$).

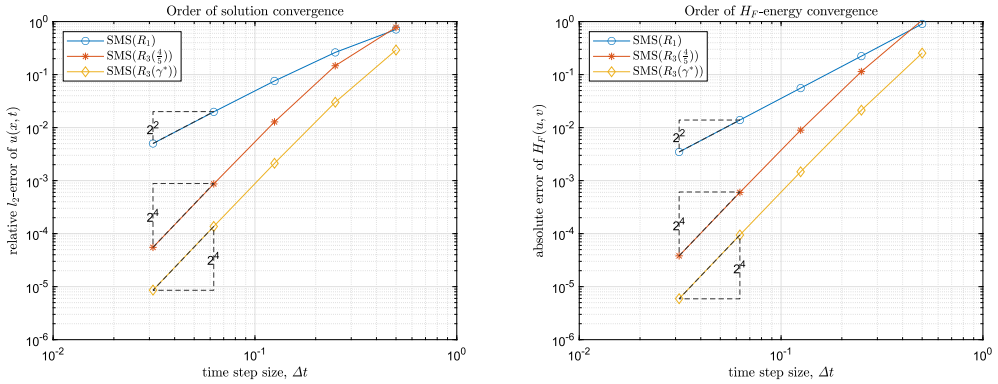

Fig. 10. Convergence of the solution and computational errors of $\mathcal{H}_F(u,v)$ at $t = 16$.

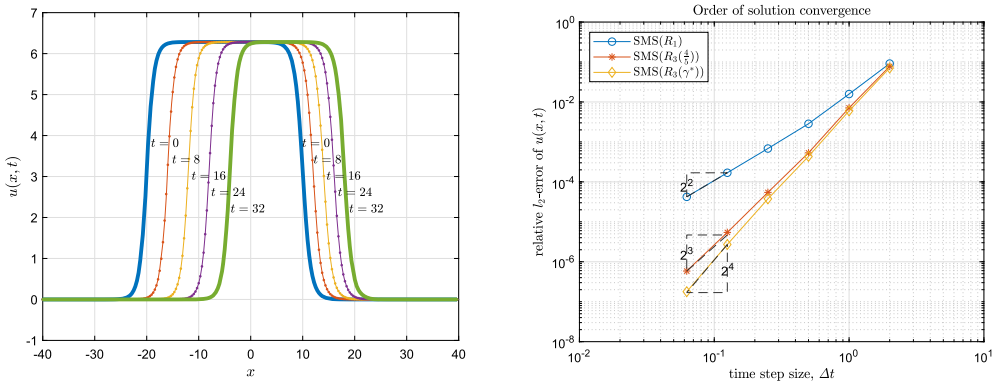

Fig. 11. Evolution of the solution and order of convergence at $t = 16$.

5.2. A Boussinesq-type equation

The Boussinesq-type equation [19],

$$u_{tt} + \Delta\left(\Delta u + 3u^2 - u\right) = 0 \tag{65}$$

is a spatially fourth-order partial differential equation in the form of (57) that corresponds to the Hamiltonian functional $\mathcal{H}_F(u,v)$ with $F(u) = u^3 - \frac{1}{2}u^2$ and $\mathbf{M}(\mathbf{x}) = 1$. For the nonlinear implicit equation (58),

$$u_i + r_i^2 \Delta t^2 \Delta \mu_i = \varphi_i, \tag{66}$$

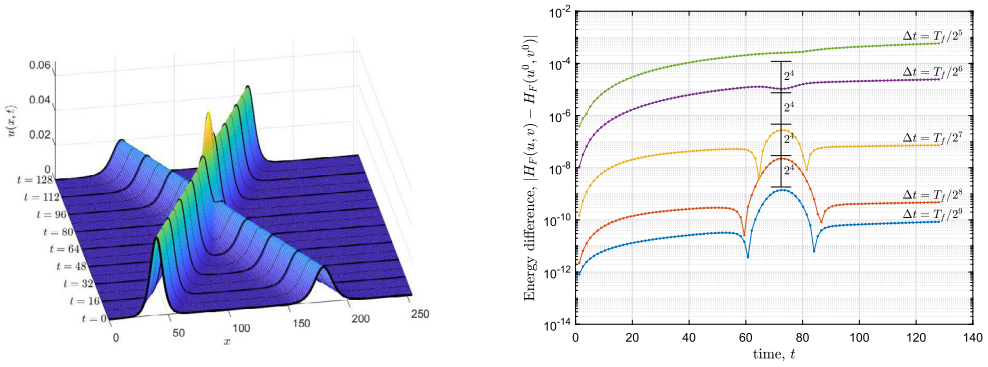

Fig. 12. Evolution of the solution and computational errors of $\mathcal{H}_F(u, v)$.

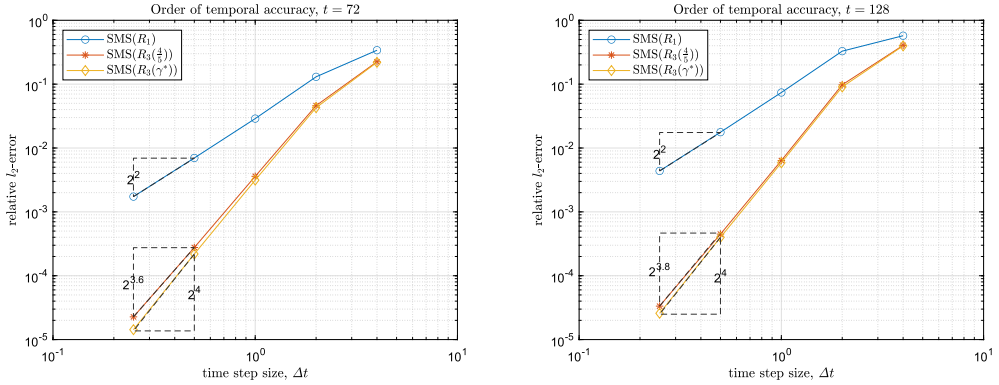

Fig. 13. Order of convergence of the solution at $t = 72$ and $t = 128$.

where $\mu_i = \Delta u_i + 3(u_i)^2 - u_i$ and $\varphi_i = u_{i-1} + \Delta t v_{i-1} + r_i^2 \Delta t^2 \Delta \mu_{i-1}$. Using the Newton-type method, we obtain an iterative solver for u_i,

$$u_i^{(m+1)} + r_i^2 \Delta t^2 \Delta \left(\Delta + 6u_i^{(m)} - 1\right) u_i^{(m+1)} = \varphi_i + 3r_i^2 \Delta t^2 \Delta \left(u_i^{(m)}\right)^2. \tag{67}$$

We consider solitary wave solutions in the form of $2b^2 \operatorname{sech}^2(b(x - x_c \pm ct))$ and numerically evolve a combination of two solitary wave-packets moving in opposite directions:

$$u(x,t) = 2b_1^2 \operatorname{sech}^2(b_1(x - x_1 - c_1 t)) + 2b_2^2 \operatorname{sech}^2(b_2(x - x_2 + c_2 t)), \tag{68}$$

where $(b_1, x_1) = (0.15, 40)$, $(b_2, x_2) = (0.1, 180)$, and $c_i = \sqrt{1 - 4b_i^2}$ is the corresponding wave speed.

For the numerical test, we set a computational domain $\Omega = [0, 256]$ with the periodic boundary condition. We choose a number of spatial discretization $N_x = 256$ that provides sufficient spatial accuracy and initial conditions as $u^0 = u(\cdot, 0)$ and $v^0 = u_t(\cdot, 0)$. Fig. 12 shows the computational solution up to $T_f = 128$ using the fourth-order SMS($R_3(\gamma^*)$) method. Again, the SMS method is no longer an energy conserving method for this quasi-linear example, but the energy $\mathcal{H}_F$ associated with the computed solution depends on $\Delta t = T_f/2^9, \cdots, T_f/2^5$. The error of the energy decays at a fourth-order rate at $t = 72$ when the two peaks merge; however, the convergence rate of the energy error shows a much better performance than the convergence order of the solution at $t = 128$.

Fig. 13 shows that the computational solution converges in the desired order of temporal accuracy (except slightly better convergence rate of SMS($R_3(4/5)$)), not only at $t = 72$ but also at $t = 128$ when the convergence rate of the energy error is higher than the expected order.

6. Conclusions

We proposed a successive multi-stage (SMS) method for the non-homogeneous linear wave equation, $u_{tt} = \nabla \cdot (\mathbf{M}(\mathbf{x}) \nabla u) + f(\mathbf{x}, t)$, which inherits the energy conservation and high-order accuracy with time. The SMS method in [16] is only for the linear wave equation, and we extend it for a case with an external force. We provided mathematical proofs of unconditional energy conservation and the unique solvability of a semi-discrete scheme and numerically demonstrated the

accuracy and energy conservation for various examples. To show the applicability of the proposed method beyond linear wave cases, we presented some examples of quasi-linear equations and demonstrated the desired order accuracy both for the solution and energy. The extension of SMS method to the quasi-linear wave or Hamiltonian partial differential equations for an energy-preserving method is the future direction of our studies.

CRediT authorship contribution statement

Jaemin Shin: Conceptualization, Numerical simulation, and Original draft writing. June-Yub Lee: Formal analysis, Validation, and Reviewing & Editing.

Declaration of competing interest

The authors declare that they have no known competing financial interests or personal relationships that could have appeared to influence the work reported in this paper.

Data availability

No data was used for the research described in the article.

Acknowledgement

This research was supported by the Basic Science Research Program through the National Research Foundation of Korea (NRF), funded by the Korean Government MSIP (2019R1A6A1A11-051177, 2020R1C1C1A01-013468).

References

[1] J. Chabassier, S. Imperiale, Introduction and study of fourth order theta schemes for linear wave equations, J. Comput. Appl. Math. 245 (2013) 194–212.
[2] J. Diaz, M.J. Grote, Energy conserving explicit local time stepping for second-order wave equations, SIAM J. Sci. Comput. 31 (3) (2009) 1985–2014.
[3] P. Joly, J. Rodríguez, Optimized higher order time discretization of second order hyperbolic problems: construction and numerical study, J. Comput. Appl. Math. 234 (6) (2010) 1953–1961.
[4] S. Britt, E. Turkel, S. Tsynkov, A high order compact time/space finite difference scheme for the wave equation with variable speed of sound, J. Sci. Comput. 76 (2) (2018) 777–811.
[5] C. Jiang, Y. Wang, Y. Gong, Explicit high-order energy-preserving methods for general Hamiltonian partial differential equations, J. Comput. Appl. Math. 388 (2021) 113298.
[6] E. Burman, O. Duran, A. Ern, Hybrid high-order methods for the acoustic wave equation in the time domain, Commun. Appl. Math. Comput. 4 (2) (2022) 597–633.
[7] T.J. Bridges, S. Reich, Numerical methods for Hamiltonian PDEs, J. Phys. A, Math. Gen. 39 (19) (2006) 5287.
[8] L. Brugnano, G.F. Caccia, F. Iavernaro, Energy conservation issues in the numerical solution of the semilinear wave equation, Appl. Math. Comput. 270 (2015) 842–870.
[9] M.A. Sánchez, C. Ciuca, N.C. Nguyen, J. Peraire, B. Cockburn, Symplectic Hamiltonian HDG methods for wave propagation phenomena, J. Comput. Phys. 350 (2017) 951–973.
[10] E. Celledoni, V. Grimm, R.I. McLachlan, D. McLaren, D. O'Neale, B. Owren, G. Quispel, Preserving energy resp. dissipation in numerical PDEs using the "Average Vector Field" method, J. Comput. Phys. 231 (20) (2012) 6770–6789.
[11] G. Quispel, D.I. McLaren, A new class of energy-preserving numerical integration methods, J. Phys. A, Math. Theor. 41 (4) (2008) 045206.
[12] H. Li, Y. Wang, M. Qin, A sixth order averaged vector field method, J. Comput. Math. (2016) 479–498.
[13] D. Furihata, Finite-difference schemes for nonlinear wave equation that inherit energy conservation property, J. Comput. Appl. Math. 134 (1–2) (2001) 37–57.
[14] T. Matsuo, D. Furihata, Dissipative or conservative finite-difference schemes for complex-valued nonlinear partial differential equations, J. Comput. Phys. 171 (2) (2001) 425–447.
[15] L. Brugnano, F. Iavernaro, D. Trigiante, Hamiltonian boundary value methods (energy preserving discrete line integral methods), J. Numer. Anal. Ind. Appl. Math. 5 (1–2) (2010) 17–37.
[16] J. Shin, J.-Y. Lee, Energy conserving successive multi-stage method for the linear wave equation, J. Comput. Phys. 458 (2022) 111098.
[17] E. Hairer, G. Wanner, Solving Ordinary Differential Equations. I, vol. 8, Springer-Verlag, Berlin, 1993.
[18] E. Hairer, G. Wanner, Solving Ordinary Differential Equations. II, vol. 14, Springer-Verlag, Berlin, 1996.
[19] H.N. Hassan, Numerical solution of a Boussinesq type equation using Fourier spectral methods, Z. Naturforsch. A 65 (4) (2010) 305–314.